ELSEVIER

Journal of Nuclear Materials 289 (2001) 247–253

journal of nuclear materials

www.elsevier.nl/locate/jnucmat

Short-time creep and rupture tests on high burnup fuel rod cladding

W. Goll [a], H. Spilker [b], E.H. Toscano [c,*]

[a] *Siemens Nuclear Power GmbH, P.O. Box 3220, 91050 Erlangen, Germany*
[b] *Gesellschaft für Nuklear-Behälter mbH, P.O.Box 101253, 45012 Essen, Germany*
[c] *European Commission Joint Research Centre at Karlsruhe, Institute for Transuranium Elements, Postfach 2340, 76125 Karlsruhe, Germany*

Received 11 September 2000; accepted 17 January 2001

Abstract

Short-time creep and rupture tests were performed to assess the strain potential of cladding of high burnup fuel rods under conditions of dry storage. The tests comprised optimized Zry-4 cladding samples from fuel rods irradiated to burnups of up to 64 MWd/kg U and were carried out at temperatures of 573 and 643 K and at hoop stresses of about 400 and 600 MPa. The applied stresses were chosen to reach about 2% strain within an envisaged testing time of 3–4 days. The tests were followed by a low temperature phase at 423 K and 100 MPa to assess the long-term behaviour of the cladding ductility especially with regard to the higher hydrogen content in the cladding of the high burnup fuel. These tests showed that around 600 K, a uniform plastic strain of at least 2% is reached without cladding failure. The low temperature phase at 423 K for up to 5 days revealed no cladding failure under these conditions of reduced cladding ductility due to the increased hydrogen content.

1. Introduction

In the last years, the discharge burnup of the light water reactor fuel has been increased continuously, among other things by introducing high corrosion resistant materials and advanced licensing methods [1]. Since dry storage is gaining more and more importance for interim storage, it is of interest to assess the creep-rupture behaviour of the zirconium cladding used for high burnup fuel rods. High burnup means increased neutron fluence and hydride content from the cladding corrosion due to long insertion times at high thermal power.

Early investigations on the mechanical properties of stress relieved and recrystallized cladding tubes have shown that burst strength and burst elongation reach a saturation level and that differences diminish at fast fluences above $4–6 \times 10^{21}$ cm^{-2} [2]. Therefore, a further increase of the fluence is not expected to have a detrimental influence on the cladding mechanical behaviour.

Hydrogen is produced during the corrosion reaction and, with increasing oxide layer thickness, an increased amount of hydrogen is found in the cladding. The properties of hydrides in zirconium and its alloys are reviewed in reference [3]. If a solubility limit of, e.g., about 150 ppm at cladding operating temperature is exceeded, the hydrogen will precipitate as zirconium hydride-platelets. The δ-phase is assumed to be the dominant phase especially under slow cooling reactor conditions. The orientation of the precipitates in the cladding will depend on texture and stress during precipitation.

The amount of hydrogen in the cladding and the orientation of the precipitates relative to the applied stress can reduce the tensile strength and the ductility compared with hydrogen-free material. At elevated

* Corresponding author. Tel.: +49-7247 951 409; fax: +49-7247 951 509.
E-mail address: toscano@itu.fzk.de (E.H. Toscano).

0022-3115/01/$ - see front matter
PII: S0022-3115(01)00438-X

temperatures (above 473 K) the effect of hydrogen on the ductility is less pronounced than it is at room temperature [4–7]. In case of irradiated materials the irradiation effect dominates the ductility up to hydrogen contents of at least 1000 ppm [8].

With regard to interim dry storage, a certain range of operational parameters has to be considered [9]. Depending on the irradiation and cask storage conditions, the maximum cladding stresses are 100–120 MPa at the beginning of storage and the temperature ranges from 673 K down to 473 K after some tens of years. This means that the cladding is mainly operated in a regime of low hydride reorientation (<100 MPa) and above the ductile–brittle transition (>200°C) [3].

The short-time creep tests were supplemented by creep tests on unirradiated cladding materials. The aim of these tests was to provide conservative limits for the post-pile creep of irradiated cladding (i.e., unirradiated cladding creep properties, to prevent fuel rod degradation by limiting the cladding hoop strain to values within these limits [10]).

The short-time creep testing on irradiated cladding was geared to demonstrate the strain capability of high burnup cladding and the cladding integrity under realistic hydrogen concentrations. Therefore, the experiment was divided into two different stages. The first stage consisted of a creep test covering the relevant temperature range of dry storage. It was performed with the objective of reaching a plastic hoop strain of about 2% within few days: this is much faster than under conditions of dry storage at typical storage temperatures of 573 and 643 K. The creep test was followed by a ductility test in which the cladding was slowly cooled down to 423 K and held at a stress of 100 MPa up to 5 days. These high stress levels and relatively low temperatures constitute one of the most severe cases under intermediate storage conditions.

2. Materials and irradiation behaviour

The cladding material used in the tests was prepared from two standard fuel rods with an outer diameter of 10.75 mm and a wall thickness of 0.73 mm. The cladding consisted of corrosion-optimized Zircaloy-4 with 1.29 w/o Sn, 0.22 w/o Fe, and 0.12 w/o Cr. The annealing parameter [11] was about 2.2×10^{-17} h. In the as-fabricated state, the cladding had a tensile strength of 78 MPa at room temperature and of 42 MPa at 673 K.

The rods, identified as A and B, were irradiated in a commercial PWR for four and five irradiation cycles up to rod average burnups of 54 and 64 MWd/kg U equivalent to neutron fluences of 9.5×10^{21} and 12.1×10^{21} cm^{-2} ($E_n > 1$ MeV), respectively. The irradiation behaviour of the rods was deduced from non-destructive examinations performed on rod B and on comparable rods.

The diameter change of rods from the same batch is shown in Fig. 1 as a function of the burnup. It can be seen that the cladding of rod A experienced a maximum diameter decrease (creepdown) of 0.8–0.9%, whereas cladding of rod B has undergone subsequently creep-back of about 0.2%. Fig. 2 shows the axial oxide layer profiles of the rods. The oxide layer of rod B was measured non-destructively by the eddy current technique (accuracy ±3 μm) and circumferentially averaged over an axial length of 40 mm. The axial oxide layer profile of rod A was estimated from a comparable oxide layer profile that was adjusted by means of oxide layer thicknesses obtained metallographically at three axial rod positions to within the same order of accuracy as the eddy current technique.

It can be seen that rod A had an oxide layer thickness up to 47 μm and rod B a layer thickness up to 100 μm.

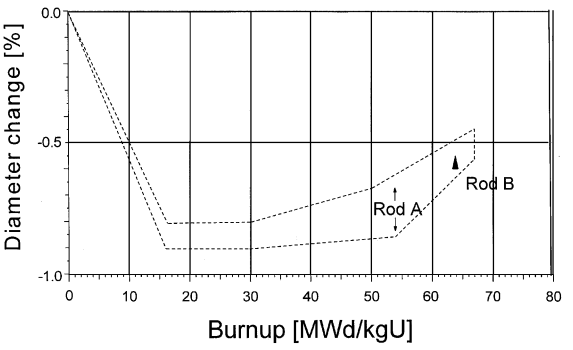

Fig. 1. Diameter behaviour of the cladding during reactor operation.

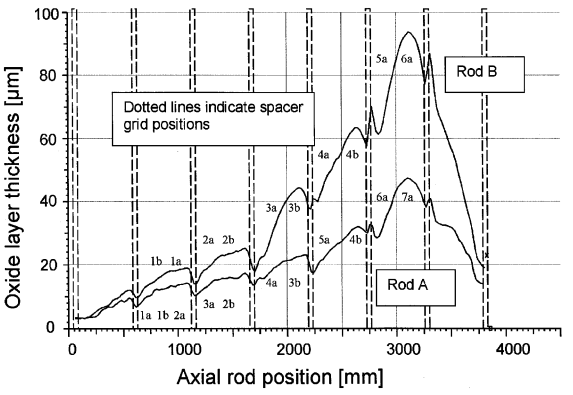

Fig. 2. Axial oxide layer thickness of rods A and B as a function of axial position and sample locations.

3. Experimental

3.1. Equipment design

The system is based on the internal pressurization of a cylindrical sample and is able to perform creep- as well as burst-tests. Oil pressurization (stiff system) was preferred to gas pressurization (soft system) because its intrinsic lower stored energy, enabling more accurate post-test measurements of the cladding deformation. In Fig. 3 a schematic diagram of the apparatus is shown. The system, reaching pressures up to about 200 MPa, is situated outside the hot cell and is connected to the sample in the hot cell through a pipeline system.

The dual piston pump allows a constant rate of pressure increase in the sample. The pumping rate can be varied in order to avoid that a pressure surge will be produced during a pump stroke or the overloading of the system due to inertia. During the test, a computer controls the pump; the pumping rate is set to the minimum and the software assures a constant pressure to within ±0.1 MPa during the whole test.

A data-logging system allows the simultaneous recording of: (i) the specimen pressure, as measured by a pressure transducer located near to the sample, (ii) the oil volume input to the specimen, obtained from the piston travel via a potentiometer transducer, and (iii) the temperature of the sample. At pre-set intervals (usually every 10 min), the instantaneous values of the pressure, temperature and piston displacement can be recorded during the whole test.

A silicon oil (Dow Corning 200) was used, as pressurization fluid having a cubic thermal expansion coefficient of 1.34×10^{-3} K^{-1} and a compression coefficient ($\Delta V/V_0$) of about 0.2 at room temperature. In the closed system used, the stability of the oil was not affected by the temperature and no cracking and/or oxidation phenomena were observed.

An electrical furnace, having three heating zones and provided with an internal double wall lining containing Cs, allows the homogeneous heating of the sample to the test temperatures. During the test, a temperature difference along the whole sample length of less than ±0.2°C could be achieved. The temperature gradient is checked by means of two thermocouples attached to the upper and lower grips and a third one positioned near to the center of the sample. The temperature control system achieves an accuracy better than ±2°C.

The equipment was designed for samples, having variable diameter up to 150 mm in length which, taking into consideration the grip length, ensures an unsupported length of about 10 times the average outside diameter, as recommended in the ASTM – Norm B 353.

3.2. Ancillary equipment

Three devices were developed in order to (a) remove the fuel, (b) tighten the specimen grips and (c) measure the sample diameter, before and after the testing.

3.2.1. Fuel removal and sample preparation

Based on a commercial drilling machine with hammer action, a device was developed to remove the fuel from the segments of irradiated fuel rods, Fig. 4. The device uses a hard metal drilling tool, fixed during the

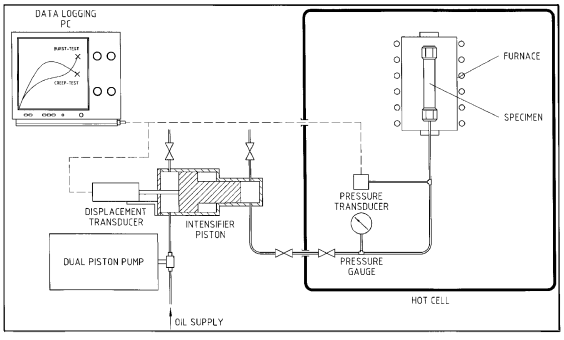

Fig. 3. Scheme of the creep test setup.

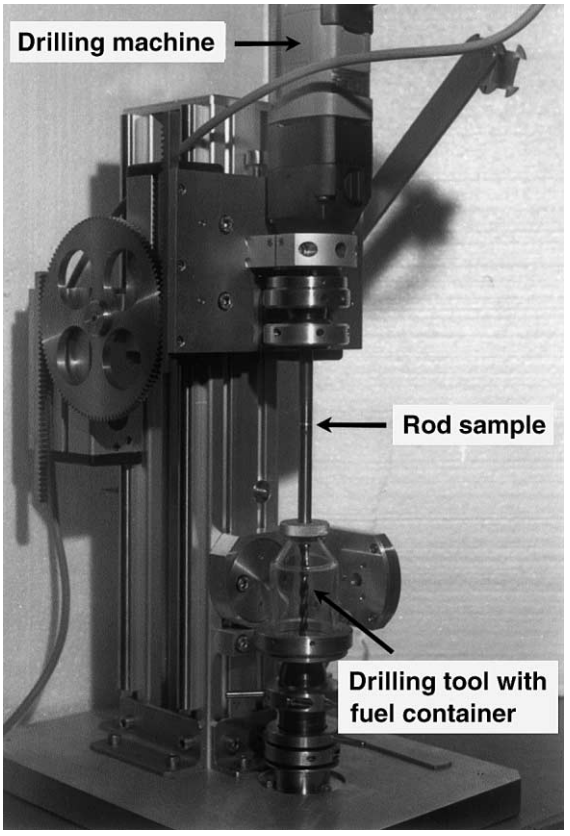

Fig. 4. Fuel removal device.

operation while the rotating fuel rod sample is displaced down onto the fixed drill bit. The system allows a smooth vertical displacement through counterweights, which maintain the sample in quasi-equilibrium.

The diameter of the drilling tool was around 1 mm smaller than the nominal internal diameter of the sample. Considering that the fuel-cladding interaction at the burnups of interest (more than 50 GWd/t U) can be large, an additional technique was developed to partially remove the interaction layer in the grip zones. To this goal, a lathe modified for use under remote controlled conditions and provided with special grinding tools was used (see below).

3.2.2. Tightening device

Mechanically attached end-fittings were used to seal the specimen. In order to screw the fittings, a special device was developed on the basis of a commercial pneumatic wrench, able to perform a smooth tightening of the fittings, thereby avoiding impacting of pulsing tightening cycles which could lead to the damage of the samples. The maximum achievable torque is around 500 N/m.

The torque can be controlled to within $\pm 5\%$ by regulating the gas pressure. The samples were strengthened by inner mandrels in order to support, at least partially, the external forces applied during the tightening of the metallic seals. The mandrels are provided with a groove to facilitate the displacement of the fluid within the specimen.

3.2.3. Sample measurement

A displacement transducer (LVDT) has been mounted on a floating head to measure the relative movement of two knives, which use as reference calibrated standards. The device is able to detect variations of ± 0.1 μm in the diameter. The apparatus also performs the measurement of the axial displacement (± 10 μm), allowing the correlation of the diameter measurement with the axial position on the sample.

3.3. Specimen preparation

Special care was exercised during the drilling operation to avoid damage of the sample wall or to cause the deformation of the sample. Drilling periods were alternated with pauses, to avoid the sample heat-up during the drilling procedure.

A lathe was used to remove the remaining fuel and, partially, the interaction layer. The internal diameter of the sample was then measured by calibrated gauges and the value used to machine the internal mandrel with a typical tolerance of about 20 μm. Finally, the fuel segments were externally treated with a fine emery paper and visually inspected to ascertain that neither undercuts nor scratches were present on the surface. Finally before the test, the samples were usually measured in five axial and in four azimuthal positions, to determine possible eccentricities.

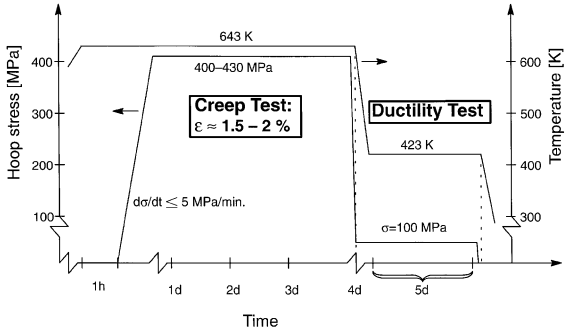

Fig. 5. Testing sequence.

3.4. Creep tests

It was necessary to establish a precise schedule for the tests. This schedule included (a) the pre-loading (about 50 MPa) of the sample during the heating phase, in order to avoid the seeding of the oil in the sample; (b) a careful elimination of the occluded air, to keep the stored energy low and to have a reliable measurement of the strain through the amount of oil pumped into the sample; (c) the pressurization of the creep samples was performed only after the test temperature was achieved and remained stable; and (d) a pre-heating phase at low pressure (50 MPa), lasting 2 h.

Fig. 5 shows the schematic sequence of the tests for a maximum temperature of 643 K. The test with a maximum temperature of 573 K was carried out under the same conditions. Both tests were designed to reach a plastic hoop strain of about 2% within 3–4 days. The appropriate pressure was chosen accordingly and the sample pressurized with a rate of less than 35 MPa/min. The strain rate was determined from the change of the oil inventory and the pressure was slightly corrected if necessary.

In case of intact samples, the creep phase was followed by a ductility test at 423 K and reduced cladding stresses as compared to the creep phase (100 MPa). The ductility test lasted about 5 days.

4. Results

The results of the creep tests on the rods A and B are presented in Tables 1 and 2. The cladding stress needed to achieve the required creep rate was in the range 400–430 MPa at 643 K and of about 600 MPa at 573 K. At 643 K the samples reached uniform plastic elongations between 0.3% and 7.4%. The low value of 0.3% resulted

Table 1
Results of the creep tests on rod A samples

Rod designation	Test conditions		Uniform plastic elongation (%)	Ductility test at 100 MPa, 423 K, time (h)	Comment
	Stress (Mpa)	Time (h)			
	Temp. 643 K				
A 1a	320	72	4.5	90	Sample intact
A 2a	430	30	7.4	100	Sample intact
A 3a	430	2	0.3		Clamping failed
A 4a	430	54	4.2	62	Sample intact
A 5a	400	129	≈6[a]		Sample failed
A 6a	410	74	2.3	89	Sample intact
A 7a	410	67	≈4.5[a]		Sample failed
	Temp. 573 K				
A 1b	630	65	1.2		Clamping unstable
A 2b	620	44	1.0	109	Sample intact
A 3b	620	189	2.4	26	Sample intact
A 4b	620	69	3.5	92	Sample intact

[a] Averaged over intact region.

Table 2
Results of the creep tests on rod B samples

Rod designation	Test conditions		Uniform plastic elongation (%)	Ductility test at 100 MPa, 423 K, time (h)	Comment
	Stress (MPa)	Time (h)			
	Temp. 643 K				
B 1a	400	100	2.5	90	Sample intact
B 2a	400	124	3.1	63	Sample intact
B 3a	420	111	4.1	119	Sample intact
B 4a	410	137	4–6[a]		Sample failed
B 5a	400	88	≈5[a]		Sample failed
B 6a	410	55	3.0		Sample failed
	Temp. 573 K				
B 1b	620	143	1.9	120	Sample intact
B 2b	620	143	1.1	97	Sample intact
B 3b	620	119	1.4		Defect near clamping
B 4b	630	13	⩾2.5		Repaired sample failed

[a] Averaged over intact region.

from an early defect in the clamping region. At 573 K the range of uniform plastic elongation was 1.0–3.5%. In the case of the lower temperature, it was difficult to maintain the tightness of the clamping for a sufficiently long time.

The results are plotted in Fig. 6. It can be seen that no cladding failure occurred below 2% uniform plastic strain. Above 2% elongation, rupture was observed on 6 out of 15 samples. Before failure, the elongation versus time curve derived from the oil inventory always showed that the samples were in the ternary creep stage, Fig. 7. This is an indication for high local ductility of the cladding. A systematic influence of the oxide layer on the creep behaviour could not be detected. However, since the hydrogen content (in this

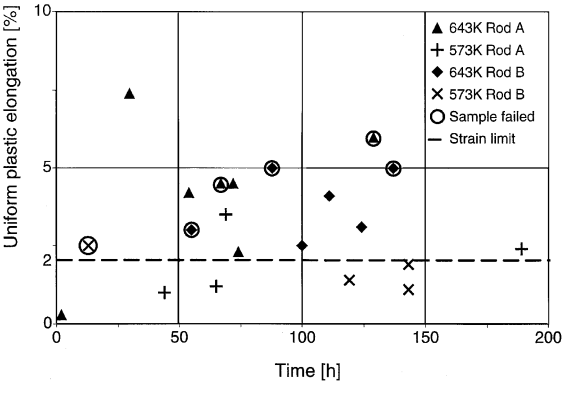

Fig. 6. Uniform plastic strain as function of testing time.

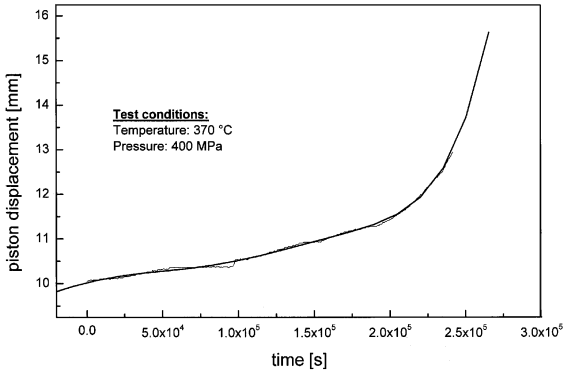

Fig. 7. Piston displacement as a function of time until sample rupture.

case amounting to several hundred ppm) is directly correlated with the oxide layer thickness, it can be deduced that the hydrogen content does not play a significant role in the creep behaviour under the present conditions.

All intact samples were submitted to a ductility test at 423 K to test influence of hydrogen at low temperatures and the effects of cladding stresses comparable to those found in high burnup rods due to their internal pressure. All samples tested remained intact.

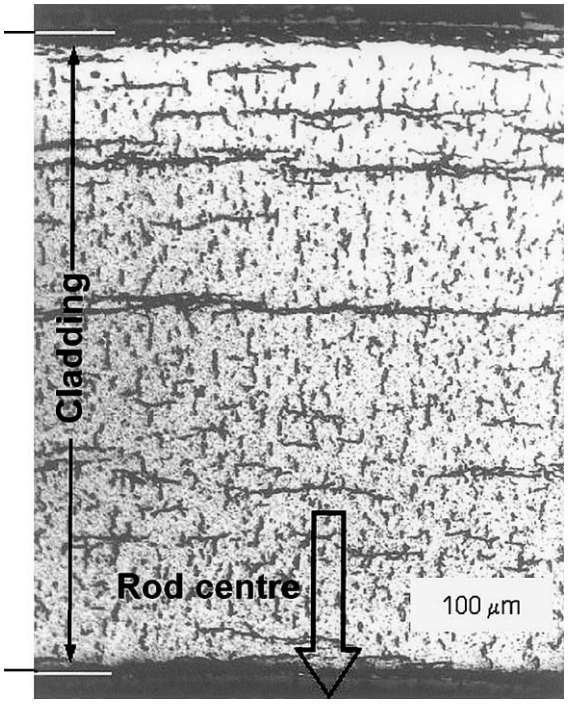

Fig. 8. Metallographic examination of sample A 3b after 573 K – creep and 423 K – ductility testing.

The behaviour of hydrogen in the cladding was investigated by metallographic examinations performed after testing. Fig. 8 shows the hydride distribution of the intact sample A 3b tested at 573 K. The tangentially oriented platelets (horizontal in photo) reflect the typical distribution immediately after discharge from the reactor.

During testing at 573 K part of the platelets were dissolved and precipitated under stress (100 MPa) during the cool-down phase of about 3 h for the ductility test. This led to the precipitation of radially oriented platelets, however, without cladding failure.

The short-term creep and rupture tests have shown that corrosion-optimized Zry-4-cladding of high burnup fuel rods can reach 2% plastic strain under the very high stresses of 400–600 MPa. That the samples can undergo such a high strain without cladding degradation proves that a comfortable margin exists in its mechanical properties, especially with regard to a licensed level of 1% [12]. This is also valid for other cladding types with base materials of lower creep rates since the creep model is a general one and was validated with an enveloping fast creep rate material.

5. Conclusions

Short-term creep and rupture testing has been carried out on corrosion-optimized Zry-4 claddings from high burnup rods (54–64 GWd/t U) irradiated in LWR reactors and has shown that the necessary 1% plastic strain for cask-licensing is clearly achieved by these rods.

Cladding material with a realistic hydrogen distribution was tested under simulated low-ductile conditions, i.e., cladding stress of 100 MPa and a temperature of 423 K. For dry storage conditions this combination of high stress and relatively low temperature is very unlikely to be reached. Nevertheless, even under these severe conditions, no hydrogen-induced degradation could be detected.

Acknowledgements

We are grateful for the funding by the German utilities. We would like to thank the utility group ‘Fuel Assembly Cladding Behavior’ for the fruitful cooperation and useful discussions.

References

[1] H. Gross, P. Urban, TOPFUEL ’99, Avignon, France, p. 262.

[2] F. Garzarolli, R. Manzel, H. Schönfeld, E. Steinberg,, Sixth SMIRT Conference, Paris, 1981, C2/1.
[3] D.O. Northwood, U. Kosasih, Int. Metals Rev. 28 (1983) 9.
[4] D.S. Wood, J. Winton, B. Watkins, Electrochem. Technol. 4 (1966) 250.
[5] G.D. Fearnehough, A. Cowan, J. Nucl. Mater. 22 (1967) 137.
[6] J. Bai, C. Prioul, J. Pelchat, F. Barcelo, ANS/ENS Topical Meeting on Light Water Reactor Fuel Performance 1991, p. 233.
[7] S.-Q. Shi, M.P. Puls, J. Nucl. Mater. 275 (1999) 312.
[8] W. Jahreiß, R. Manzel, E. Ortlieb, in: Proceedings of the Jahrestagung Kerntechnik '93, 1993, p. 303.
[9] M. Peehs, F. Garzarolli, W. Goll, International Symposium on Storage of Spent Fuel from Power Reactors, IAEA-TECDOC-1089, 1999, p. 313.
[10] H. Spilker, M. Peehs, H.-P. Dyck, G. Kaspar, K. Nissen, J. Nucl. Mater. 250 (1997) 74.
[11] E. Steinberg, H.G.Weidinger, A. Schaa, ASTM-STP 824, p. 106.
[12] W. Sowa, D. Hoffmann, B. Lorenz, in: Proceedings of the Jahrestagung Kerntechnik'98, 1998, p. 265.